Biochimica et Biophysica Acta 1857 (2016) 7–13

Contents lists available at ScienceDirect

Biochimica et Biophysica Acta

journal homepage: www.elsevier.com/locate/bbabio

Unraveling the electron transfer processes of a nanowire protein from *Geobacter sulfurreducens*

Mónica N. Alves [a,1], Ana P. Fernandes [a,b,1], Carlos A. Salgueiro [b], Catarina M. Paquete [a,*]

[a] Instituto de Tecnologia Química e Biológica — António Xavier, Universidade Nova de Lisboa, Oeiras, Portugal
[b] UCIBIO-Requimte, Departamento de Química, Faculdade de Ciências e Tecnologia, Universidade NOVA de Lisboa, Caparica, Portugal

ARTICLE INFO

Article history:
Received 10 July 2015
Received in revised form 4 September 2015
Accepted 30 September 2015
Available online 3 October 2015

Keywords:
Multiheme cytochromes
Geobacter
Nanowires
Electron transfer
Extracellular respiration

ABSTRACT

The extracellular electron transfer metabolism of *Geobacter sulfurreducens* is sustained by several multiheme *c*-type cytochromes. One of these is the dodecaheme cytochrome GSU1996 that belongs to a new sub-class of *c*-type cytochromes. GSU1996 is composed by four similar triheme domains (A–D). The C-terminal half of the molecule encompasses the domains C and D, which are connected by a small linker and the N-terminal half of the protein contains two domains (A and B) that form one structural unit. It was proposed that this protein works as an electrically conductive device in *G. sulfurreducens*, transferring electrons within the periplasm or to outer-membrane cytochromes. In this work, a novel strategy was applied to characterize in detail the thermodynamic and kinetic properties of the hexaheme fragment CD of GSU1996. This characterization revealed the electron transfer process of GSU1996 for the first time, showing that a heme at the edge of the C-terminal of the protein is thermodynamic and kinetically competent to receive electrons from physiological redox partners. This information contributes towards understanding how this new sub-class of cytochromes functions as nanowires, and also increases the current knowledge of the extracellular electron transfer mechanisms in *G. sulfurreducens*.

1. Introduction

C-type cytochromes are among the most diverse classes of metal-containing proteins, fulfilling various functions in numerous biological electron transfer processes [1]. The heme groups are covalently linked to the polypeptide chain through thioether bonds set by the cysteine residues in the heme-binding motif Cys-X-X-Cys-His. In this motif, the histidine is usually one of the axial ligands to the heme iron and X can be any amino acid residue. Interestingly, the covalent attachment to the polypeptide chain allows *c*-type cytochromes to bind numerous hemes on a short stretch of protein, where the heme–protein ratio is high and only very little secondary structure can be observed. In dissimilatory metal reducing bacteria (DMRB) multiheme *c*-type cytochromes (MHC) are implicated in several processes, such as electron transfer in respiratory processes [2,3], gene regulation [4] and as electron-storage sinks or capacitors [5,6].

The genome of the Gram-negative δ-proteobacterium *Geobacter sulfurreducens* [7] contains three ORFs encoding two proteins with 12 heme binding sites (GSU0592 and GSU1996) and one with 27 heme binding motifs (GSU2210). Homologous polymers were also found in the genome of *Geobacter metallireducens* and *Geobacter uraniireducens*, with pairwise sequence identities higher than 70%, leading to the establishment of a new sub-class of cytochromes [8]. The crystal structure of GSU1996 cytochrome was recently determined and showed that these cytochromes are formed by highly homologous triheme domains that are connected to each other by short linkers [9]. Each module shares similarities with the triheme cytochrome c_7 that can be found in several MHC from *Geobacter* spp. [8]. In each of these c_7-type domains, the hemes I and III, numbered by analogy to the structurally homologous hemes of tetraheme cytochromes c_3 [10], present bis-histidinyl axial coordination, while heme IV contains a histidine and a methionine axial ligands [8,9].

The structure of GSU1996 revealed a novel architecture that spans about 12 nm end to end and contains 12 hemes. The C-terminal half of the molecule consists of two c_7-type domains (domains C and D) that are connected by a flexible linker, while the N-terminal half of the protein has the two c_7-type domains A and B organized as an elongated structural unit [9]. Interestingly, the heme–heme distances are within van der Walls interaction distances, enabling efficient electron exchange between them. For this reason, it was proposed that this protein may function as a natural "nanowire" transferring electrons within the periplasmic space of *Geobacter sulfurreducens* [9]. It was also proposed that in the absence

Abbreviations: DMRB, dissimilatory metal reducing bacteria; MHC, multiheme cytochromes; NMR, nuclear magnetic resonance.

* Corresponding author at: Instituto de Tecnologia Química e Biológica António Xavier, Universidade NOVA de Lisboa, Av. da República — EAN, 2780-157 Oeiras, Portugal.
E-mail address: cpaquete@itqb.unl.pt (C.M. Paquete).

[1] These authors contributed equally to this publication.

http://dx.doi.org/10.1016/j.bbabio.2015.09.010
0005-2728/

of electron acceptors, these proteins contribute to the enhancement of the cellular electron-storage capacity. In this process, they may receive electrons from the inner-membrane and contribute to prevent metabolic arrest [5].

In order to understand if this new sub-class of cytochromes functions as a nanowire or as an electron-storage capacitor it is necessary to elucidate their electron transfer processes. This information is only possible with a detailed characterization of the thermodynamic and kinetic properties of the various redox centers [11]. While the thermodynamic data allow identification of the possible electron transfer pathways, the kinetic properties elucidate the velocity of a particular electron transfer event and define the electron transfer steps that occur in the protein. Over the years, methodologies that discriminate the individual redox properties of multiple centers and their pairwise interactions were developed [11]. These methods are of general application and independent of any structural organization of the proteins.

In this work, the thermodynamic and kinetic properties of the fragment CD of GSU1996 were determined and used to elucidate the electron transfer processes performed by the C-terminal half of the protein GSU1996 for the first time. This extends the experimental application of methods that define microscopic properties of multicenter redox proteins to a case of six redox centers with a significant functional role. It was shown that the most exposed heme of domain D, at one edge of the protein, is the most thermodynamic and kinetically competent to receive electrons from the redox electron donor, and allows the protein to work as a nanowire device. This information is pioneer and contributes significantly to the understanding of the mechanisms of long-range electron transfer along these nanowire cytochromes.

2. Materials and methods

2.1. Protein purification

The GSU1996 domains C and D, as well as the fragment CD, were expressed and purified as previously described [8,12] with minor changes. Briefly, the proteins were produced in *Escherichia coli* strains JCB7123 (domain C) [13] and JM109 (domain D and fragment CD) harboring plasmid pEC86, which contains the *c*-type cytochromes maturation gene cluster *ccmABCDEFGH* [14].

The overexpressed proteins were purified as follows: the periplasmic fractions were isolated by osmotic shock in the presence of lysozyme (Sigma-Aldrich) and dialyzed against 10 mM Tris–HCl pH 7.0 (domains C and D) or 20 mM sodium phosphate pH 5.9 (fragment CD). Subsequently, the samples were subjected to two chromatographic steps. In the first step, samples were separately loaded onto cation-exchange columns (Econo-Pac High S, Bio-Rad) and eluted with a linear gradient of NaCl. In the second step, the fractions containing the proteins of interest were pooled, concentrated and loaded onto a HiLoad 16/60 Superdex 75 column (GE Healthcare), equilibrated with 20 mM sodium phosphate pH 8.0 buffer containing 100 mM NaCl. Both chromatographic steps were performed in an ÄKTA Prime Plus FPLC System (GE, Amersham). The presence of the purified proteins was confirmed by sodium dodecyl sulfate polyacrylamide gel electrophoresis (12% SDS-PAGE) with both heme [15] and Coomassie blue staining. Protein concentrations were determined by UV–visible spectroscopy using the specific absorption coefficient of the α-band at 552 nm determined for the reduced cytochrome c_7 PpcA ($\varepsilon_{552\ nm} = 32.5\ mM^{-1}\ cm^{-1}$ per heme) [16].

2.2. NMR experiments

The buffer of the purified proteins was exchanged for 80 mM sodium phosphate buffer (pH 8.0) with NaCl (final ionic strength of 250 mM) prepared in 99.9% ^2H_2O (CIL), through ultrafiltration procedures with Amicon Ultra Centrifugal Filter Units (Millipore). Protein samples with approximately 1.5 mM were placed in 3 mm Wilmad NMR tubes. The 1D ^1H NMR spectra were acquired on a Bruker Avance 600 MHz spectrometer with a spectral width of 30 kHz at 289 K. ^1H chemical shifts were calibrated using the water signal as internal reference. All NMR spectra were processed using TopSpin™ NMR Software from Bruker Biospin.

2.3. Redox titrations followed by visible spectroscopy

Redox titrations of domain D and fragment CD followed by UV–visible spectroscopy were performed at 289 K in anaerobic conditions as described previously in the literature [16]. Protein solutions were prepared in 80 mM phosphate buffer (at pH 7 and 8) with NaCl (final ionic strength of 250 mM) inside an anaerobic glove box (MBraun), kept at below 2 ppm oxygen. To ensure equilibrium between the electrode and the redox centers of the protein, a mixture of redox mediators was used: indigo tetrasulfonate, indigo trisulfonate, indigo disulfonate, riboflavin, anthraquinone 2-sulfonate, safranin, benzyl viologen, neutral red, and methyl viologen. For redox titrations performed at pH 7, the mediator 2-hyroxy 1,4-naphthoquinone was added to the redox mediators mixture, while for redox titrations performed at pH 8 the mediators methylene blue and gallocyanine were added to the redox mediators mixture. Different concentration ratios of protein (approximately 10 μM) to mediators (between 1 and 2 μM) were tested to check for possible interactions between the protein and redox mediators. To check for hysteresis and reproducibility, the redox titrations were repeated at least twice in the oxidative and reductive directions for each pH. The reduced fraction of the cytochromes was determined by calculation of the area of the α peak using the absorbance data obtained at 552 nm and the isosbestic points of the target proteins. This analysis allows the subtraction of the optical contribution from the redox mediators.

2.4. Reduction kinetic experiments with sodium dithionite

Kinetic data were obtained by measuring the light absorption changes at 552 nm with a stopped-flow instrument (SHU-61VX2 from TgK Scientific) placed inside the anaerobic chamber. The temperature of the kinetic experiments was kept at 289 ± 1 K using an external circulating bath.

The reduction experiments were performed by mixing the target proteins with sodium dithionite. The target proteins were prepared in degassed 80 mM phosphate buffer (pH 7 and 8) with NaCl (final ionic strength of 250 mM). In order to guarantee pseudo-first order conditions (see below), this strong reducing agent was used in large excess [17]. Solid dithionite was added to degassed 5 mM phosphate buffer pH 8 with NaCl (final ionic strength of 250 mM). The concentration of the reducing agent was determined in each experiment using $\varepsilon_{314\ nm}$ of 8000 $M^{-1}\ cm^{-1}$ [18]. Partially reduced protein was prepared by adding small amounts of concentrated solution of sodium dithionite to achieve the desired degree of reduction, before the beginning of the kinetic experiment. The reference value for the absorbance of the fully oxidized state of the protein was obtained at 552 nm in the beginning of the experiment by mixing the oxidized protein with degassed buffer, while the reference value for the fully reduced state of the protein was obtained from the final absorbance taken at effectively infinite time.

For the three proteins, the reducing agent was found to be the one-electron donor bisulfite radical ($SO_2^{\bullet}$) [19]. The pH of the samples was measured after each kinetic experiment and was taken as the pH of the kinetic experiment.

2.5. Data analysis

2.5.1. Thermodynamic analysis

The model used in the analysis was adapted from the thermodynamic model previously developed [11,20]. For a protein with six

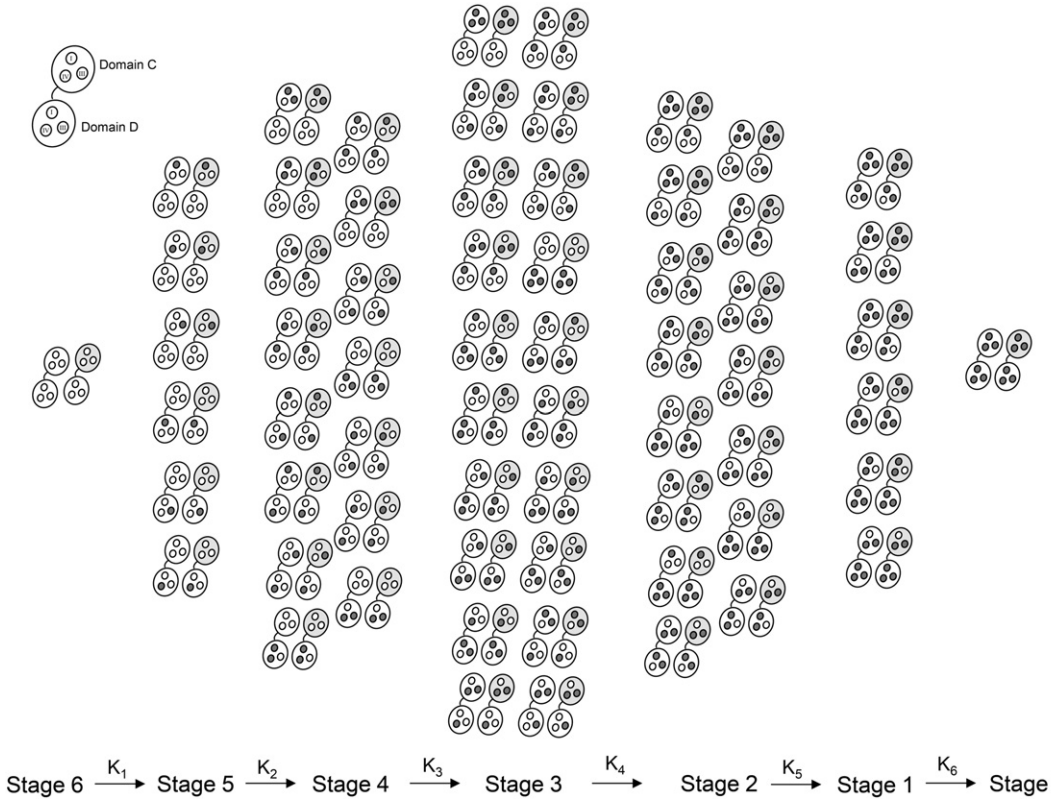

Scheme 1. Schematic representation of the microstates of fragment CD from GSU1996, a protein with six hemes and one acid–base center. The protein is represented as large circles, with black and white dots representing the hemes in the reduced and oxidized state, respectively. White and gray protein represents the deprotonated and protonated microstates for the acid–base center associated with the hemes. The redox stages are numbered according to the number of oxidized hemes and organized in columns that group populations with the same oxidation state. Macroscopic electron transfer steps between stages are shown in the direction of reduction, and macroscopic rate constants are represented by K_{1-6}.

hemes and one protonable center, such as for the fragment CD, 64 microstates are necessary to describe in detail all possible redox transitions (Scheme 1).

The microscopic thermodynamic parameters of this protein include 6 reduction potentials, one for each heme, the pK_a of the ionizable center, 15 redox interaction energies between the heme groups, and 6 redox-Bohr interaction energies between the hemes and the ionizable center [11]. The thermodynamic model considers that the redox interactions between each pair of hemes are only due to Coulombic effects, and that no conformation modification occurs with reduction or

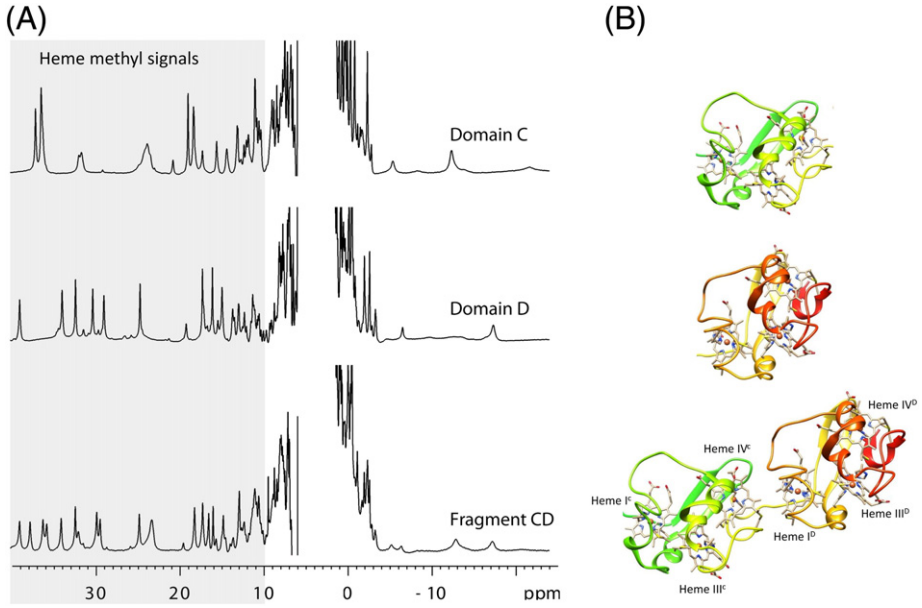

Fig. 1. (A) 1D ^{1}H NMR spectra of domains C, D and of fragment CD from *G. sulfurreducens* at 289 K and pH 8. The NMR spectral region where heme methyl groups of low-spin *c*-type cytochromes appear are highlighted by a gray box. (B) Three-dimensional structures of domain C, domain D and fragment CD. The 3D structures of domains C and D were taken from the 3D structure of the fragment CD (pdb: 3OUE). The hemes are numbered by analogy to the structurally homologous hemes in tetraheme cytochromes c_3.

Table 1
Heme redox interaction energies of domain D in fragment CD from GSU1996. These values were determined from the Debye–Hückel model of shielded electrostatic interactions (see Materials and methods).

	Heme pairs	Distance (Å)	Interaction energies (meV)
Fragment CD	I^D–III^D	11.3	34
	I^D–IV^D	18.0	9
	III^D–IV^D	12.1	29
	I^C–I^D	30.7	1
	I^C–III^D	40.6	0
	I^C–IV^D	48.3	0
	III^C–I^D	21.8	5
	III^C–III^D	30.4	1
	III^C–IV^D	39.5	0
	IV^C–I^D	14.7	17
	IV^C–III^D	25.3	3
	IV^C–IV^D	32.3	1

Table 2
Microscopic thermodynamic parameters determined for fragment CD from GSU1996 in the fully reduced and protonated protein.

Hemes	Energies (meV)						
	I^C	III^C	IV^C	I^D	III^D	IV^D	Ionizable center
I^C	−106	44	7	*1*	*0*	*0*	−4
III^C		−136	40	*5*	*1*	*0*	−25
IV^C			−125	*17*	*3*	*1*	−13
I^D				−155 (7)	*34*	*9*	–
III^D					−178 (5)	*29*	–
IV^D						−113(4)	–
Ionizable center							340

Diagonal terms (in bold) represent the oxidation energies of the six hemes and the deprotonation energy for the protonable center in the fully reduced and protonated protein. The off-diagonal elements represent the redox and redox–Bohr interaction energies between the seven centers (italic elements are the heme redox interaction energies of domain D in fragment CD presented in this table). The thermodynamic properties of domain D are shown in a gray box, which includes the oxidation energies of the three hemes (in bold), and the redox interaction energies between the three centers. Standard thermodynamic expressions relate the oxidation energies and deprotonation energy with reduction potentials and pK_a, respectively. Standard errors for the three parameters extracted from fitting the model to the experimental data are indicated within brackets and were calculated from the diagonal element of the covariance matrix, considering an experimental uncertainty of 3%.

oxidation of the protein. The redox interaction energies for domain D were calculated using the Debye–Hückel model of shielded electrostatic interactions, that considers an effective dielectric constant of 8.6, a Debye length of 7.7 Å [21,22], and the iron–iron distances measured in the 3D-structure of fragment CD (pdb: 3OUE). In this model, the microscopic thermodynamic parameters of domain C that include four reduction potentials, one for each individual heme, the redox interactions between pair of hemes, the pK_a of the ionizable center, and the redox-Bohr interaction energies [16] were used to predict the thermodynamic properties of domain D and fragment CD. Since domain D does not present redox-Bohr effect in the pH range studied (see Results and discussion) no redox-Bohr interactions were considered.

The simultaneous fit of four independent redox titrations obtained at pH 7 and 8 for domain D and for fragment CD to the thermodynamic model, using the microscopic thermodynamic properties published for domain C and the redox interaction energies calculated for domain D, enabled the determination of three reduction potentials, one for each heme in domain D. The thermodynamic model was implemented in Microsoft Excel® and the Generalized Reduced Gradient resolution method of the add-in program Solver was used for the fitting. This model considers that each heme contributes equally to the change of absorbance at 552 nm. The standard errors associated with the microscopic reduction potentials determined for the hemes of domain D were estimated from the covariance matrix using an experimental uncertainty of 3% of the total optical signal of the UV–visible redox titrations.

2.5.2. Kinetic analysis

Kinetic data obtained for the reduction of domains C and D, and of fragment CD with sodium dithionite at different pH values were normalized in order to have oxidized fractions *versus* time. The timescale was corrected to account for the deadtime of the apparatus. To reduce electrical noise, a minimum of two data sets were averaged for each experimental condition. The experimental data obtained for the reduction of each protein with sodium dithionite at various pH values were fitted simultaneously using the kinetic model described in the literature [11,23] adapted for 6 redox centers. The application of this model requires fast intramolecular electron transfer and slow intermolecular electron exchange. These conditions, usually given by the short distance between the hemes, ensure that a thermodynamic re-equilibration occurs within the protein between each sequential electron transfer step. Furthermore, the fast equilibrium within microstates belonging to the same stage of oxidation (within each column in Scheme 1) and the use of large excess of reducing agent simplifies the kinetic analysis [23]. In this situation each electron transfer step is characterized by a macroscopic rate constant (K_{1-6} in Scheme 1 for fragment CD) that is parsed into the contribution of all the microscopic rate constants of the transition that participate in that step (k_i^j, where *i* is the center that is under reduction, and *j* the other center(s) already reduced). Each contribution is weighted according to the thermodynamic

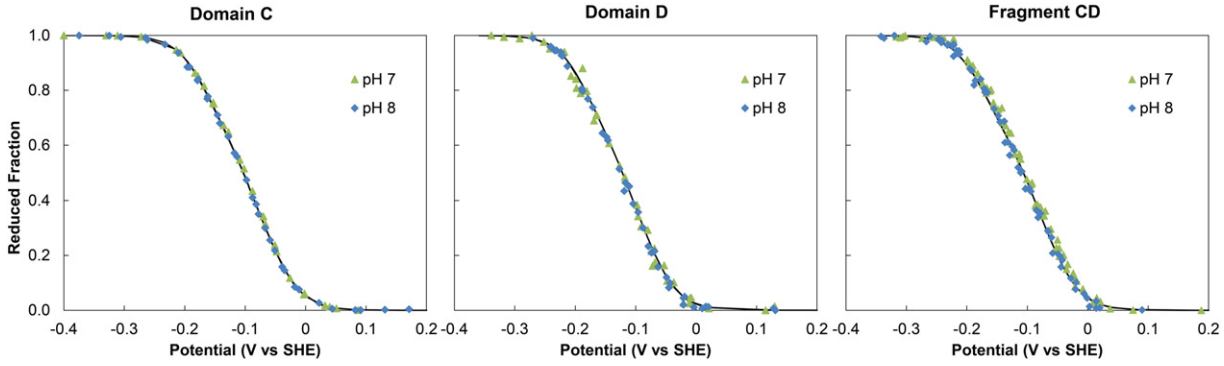

Fig. 2. Redox titrations followed by visible spectroscopy of domain C, domain D and fragment CD at pH 7 and 8 (289 K). Redox titrations of domain C were previously performed [16], whereas redox titrations of domain D and of fragment CD were performed in this work. The solid lines represent the best fit of the experimental data with the thermodynamic model described in Materials and methods section and give rise to the thermodynamic parameters reported in Table 2.

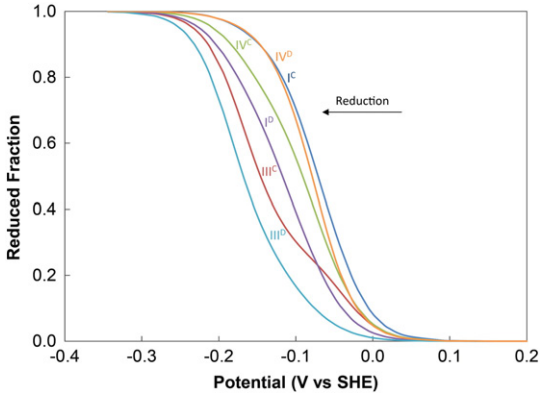

Fig. 3. Reduced fraction of the individual hemes in fragment CD from GSU1996 calculated at pH 7 with the thermodynamic parameters presented in Table 2.

equilibrium populations of the starting states, which are known from the thermodynamic properties of the protein [23]. In this model, Marcus theory for electron transfer [24] is used to separate the contribution of the driving force of the reaction from the reference rate constant (k_i^0) that is intrinsic to each heme [23]:

$$k_i^j = k_i^0 \exp\left[\frac{e_i F}{2RT}\left(1 + \frac{e_D F}{\lambda} - \frac{e_i F}{2\lambda}\right)\right].$$

In this equation e_i is the reduction potential of the transition between a particular pair of microstates and e_D is the reduction potential of the electron donor. The reference rate constants obtained with this model are intrinsic to each heme and enable the definition of the role of each heme in the overall reduction process of the protein [23].

The fitting of the experimental data was achieved using the Nelder–Mead algorithm with the kinetic model implemented in MATLAB® [25,26]. Fittings using different initial values for the reference rate constants were performed to find the best solution. An experimental uncertainty of 5% of the total amplitude of the optical signal of the kinetic trace was used to determine the standard errors associated with each reference rate constant.

3. Results and discussion

Typically, MHC contain several hemes that are closely-packed to allow efficient electron transfer within the proteins [3,27]. In the dodecaheme protein GSU1996 from *G. sulfurreducens* the hemes are arranged in a novel "nanowire" architecture, where the hemes are at close distance to each other and have substantial surface exposure [9]. Consequently, multiple centers may donate or receive electrons from the redox partners. Thus, the identification of the redox centers that contribute significantly to the intermolecular electron transfer with the redox partners is a priority to understand the functional mechanism of GSU1996. This is however only possible with the characterization of the thermodynamic and kinetic properties of the individual redox centers in the protein.

Table 3
Reference rate constants for each heme in the reduction process with sodium dithionite (k_i^0) for fragment CD from GSU1996 at 289 K. Standard errors were calculated from the diagonal element of the covariance matrix considering an experimental uncertainty of 5% of the total amplitude of the optical signal in the kinetic traces are given in parentheses.

		k_i^0 ($\times 10^6\ s^{-1}\ M^{-1}$)
Domain C	Heme I	0.0 (5.7)
	Heme III	0.0 (2.4)
	Heme IV	0.0 (5.2)
Domain D	Heme I	74.0 (2.2)
	Heme III	274.3 (1.2)
	Heme IV	0.0 (2.1)

3.1. Thermodynamic characterization of domain D and fragment CD from G. sulfurreducens

NMR can provide the spectroscopic distinction of the various hemes in a way that is highly sensitive to their redox state [28]. Indeed, in conditions of slow intermolecular and fast intramolecular electron exchange rates on the NMR timescale it is possible to follow NMR signals from a particular heme methyl through the oxidation stages of the protein, providing the necessary data to establish the oxidation order of the hemes [22,29]. This approach was previously used to characterize in detail the thermodynamic properties of domain C of GSU1996 [16]. The application of this methodology depends on the complexity of the system that is given by the size of the molecule, number of hemes and if the convenient electron exchange conditions are met. In the case of domain C, the decrease of temperature and increase of ionic strength were essential to achieve the slow intermolecular electron exchange regime necessary to follow the NMR signals through the different oxidation stages [16]. Unfortunately, for domain D the slow intermolecular exchange regime on the NMR time scale was not achieved in the same experimental conditions, even collecting data at a proton Larmor frequency of 800 MHz, precluding the determination of the detailed thermodynamic properties of this domain with this methodology. The complexity of the NMR spectra of the hexaheme domains of GSU1996 and of the GSU1996 itself prevents the discrimination of the NMR signals from each heme in each oxidation stage [11].

The 1D ^{1}H NMR spectra of domains C, D and of fragment CD exhibit the typical features of low-spin *c*-type cytochromes with signals from the heme methyl groups shifted to the low-field region between 10 and 40 ppm (Fig. 1). The dispersion of these signals is highly dependent on the relative orientation between neighboring hemes and on the relative orientation of the axial ligands [30].

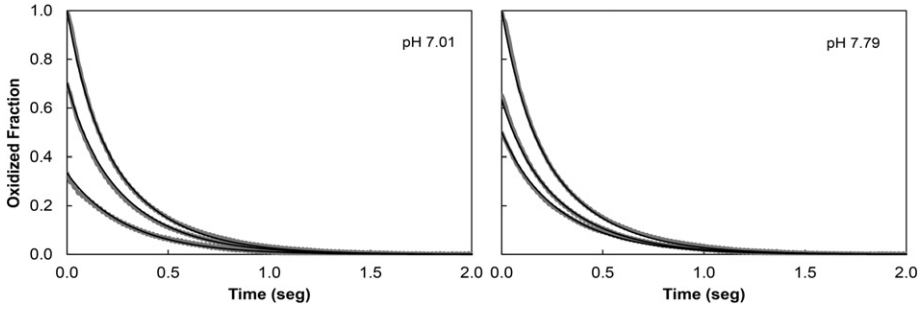

Fig. 4. Kinetics of reduction of fragment CD from GSU1996 by sodium dithionite at different pH values. Gray lines are the kinetic data obtained for the fully oxidized state of the protein, for 70% and 34% oxidized fraction at pH 7.01, and for 65% and 50% oxidized fraction at pH 7.79. Black lines are the fit of the kinetic model to the data. The concentration of sodium dithionite used in the kinetic experiments was 115 μM (after mixing), while the concentration of fragment CD was 0.91 and 0.90 μM (after mixing) at pH 7.01 and 7.79, respectively.

Table 4
Fraction of electrons that enter fragment CD from GSU1996 by each heme, calculated at pH 7 using the thermodynamic parameters from Table 2 and the reference rate constants presented in Table 3.

Stages	Hemes					
	I^C	III^C	IV^C	I^D	III^D	IV^D
Fraction of electrons	0.00	0.00	0.00	1.36	4.64	0.00

Interestingly, the 1D ^{1}H NMR spectrum of fragment CD is similar to the sum of the spectra of the individual domains, suggesting that the arrangement of the hemes and the axial ligand geometries in fragment CD are conserved. For this reason, the thermodynamic model used to characterize the properties of fragment CD considers that the redox properties of the hemes and the heme interactions among pairs of hemes are conserved in fragment CD as in the individual domains C and D. In this model the redox properties of domain C previously reported were used [16], whereas the heme interaction energies of domain D were predicted from the heme iron–iron distances (Table 1).

Redox titrations followed by UV–visible spectroscopy of domains C and D performed at pH 7 and 8 show that both proteins do not present redox-Bohr effect within the pH range (Fig. 2). Indeed, published data for domain C showed that the pK_a of the redox-linked ionizable center is lower than 6 [16]. For these reasons, the microscopic thermodynamic model only considers one ionizable center that is associated with domain C (Scheme 1).

The fitting of the redox titrations of domain D and of fragment CD to the thermodynamic model provides the reduction potential of the three hemes of domain D. Together with the published data for domain C and the calculated pairwise interactions between the hemes, the information is sufficient to achieve the detailed thermodynamic characterization of fragment CD (Table 2). Clearly, the model captures well the trend of the data and indicate that the redox behavior of the hemes in domains C and D are the same as in fragment CD (Fig. 2).

The thermodynamic parameters of fragment CD from GSU1996 show that the reduction order of the hemes are I^C, IV^D, IV^C, I^D, III^C and III^D (Fig. 3).

Interestingly, in fragment CD the heme III of both domains C and D is the last one to be reduced. In the characterization of the individual domain C heme III was shown to be the last one to be reduced [16], as it was observed for domain D (data not shown). This constitutes further evidences that the redox behavior of the individual domains is maintained in the hexaheme fragment.

3.2. Kinetic characterization of fragment CD

The kinetic traces obtained for the reduction of fragment CD from GSU1996 with sodium dithionite do not show pH dependence in the pH 7–8 range (Fig. 4). This is in agreement with the data obtained from the redox titrations monitored by UV–visible spectroscopy for fragment CD (Fig. 2). Reductive kinetic traces were obtained with the protein poised at different levels of reduction. This way, the different kinetic experiments start from equilibrium between the different stages of oxidation in a condition that depends solely on the thermodynamic properties of the hemes [17].

The kinetic model uses the thermodynamic parameters to discriminate the rate constants for the reduction of the individual hemes [23]. Table 3 presents the reference rate constants for each heme obtained by the best fit of the kinetic model to the experimental data acquired at different pH values for fragment CD. These reference rate constants are intrinsic to each heme and allow defining the contribution of each heme in the reductive process of the protein. Only hemes from domain D, in particular hemes I and III, contribute to the entrance of electrons in the fragment CD from GSU1996 (Table 4).

Interestingly, heme III, the heme that contributes more to the reduction of fragment CD (Table 4) is the most exposed heme of domain D [9] and it is the heme with the lowest reduction potential in fragment CD. Clearly, the exposure of the hemes is not the most important factor contributing for the reductive kinetic process of the protein since heme I from domain C is the most exposed heme at fragment CD [9], and does not contribute to the reduction process of the hexaheme protein.

The entrance of electrons through heme III from domain D clearly shows how GSU1996 works as a nanowire protein. Heme III from domain D, at one extreme of GSU1996, can receive electrons from the physiological electron donor and transfer them to the other hemes within the protein. Since, at least in fragment CD, this heme has the lowest reduction potential, it is spontaneously re-oxidized by the other hemes in the fragment and remains free to receive electrons from redox partners, allowing the protein to function as a nanowire device (Scheme 2).

4. Conclusion

Nanowire cytochromes are a new class of proteins found in the genome of several *Geobacter* species proposed to be responsible for long-range electron transfer. The elucidation of the detailed thermodynamic and kinetic properties of the C-terminal half of the protein GSU1996 from *G. sulfurreducens* opens the possibility to unravel the electron transfer processes performed by this new class of proteins. Indeed, the entrance of electrons through the heme that is at one edge ensures that the electrons may flow within the protein to the other end, allowing it to work as a nanowire. Further studies will enable the characterization of the full length protein, and the elucidation of the electron transfer processes during its oxidation. This information will also be of significant importance to increase our knowledge on the extracellular electron transfer processes performed by *G. sulfurreducens*, a key asset to improve its biotechnological applications, such as microbial fuel cells.

Transparency document

The Transparency document associated with this article can be found in the online version.

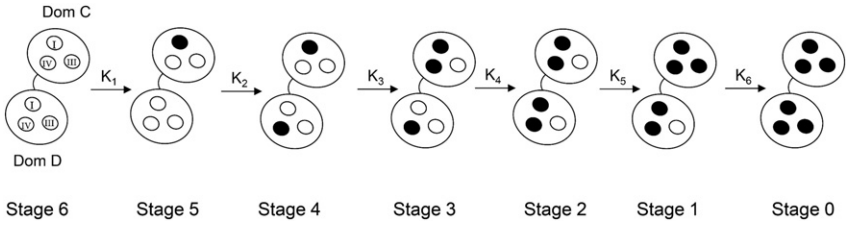

Scheme 2. Schematic representation of the most important microstates for the reduction of fragment CD from GSU1996. Black and white dots representing the hemes in the reduced and oxidized state, respectively.

Acknowledgments

The authors thank Ricardo O. Louro for his helpful discussions. This work was supported by Fundação para a Ciência e Tecnologia (FCT) Portugal [Grants PTDC/QUI-BIQ/117440/2010, UID/Multi/04378/2013; APF and CMP were supported by FCT grants SFRH/BD/86439/2012 and SFRH/BPD/96952/2013, respectively]. The NMR spectrometers are part of The National NMR Facility, supported by FCT (RECI/BBB-BQB/0230/2012).

References

[1] J. Liu, S. Chakraborty, P. Hosseinzadeh, Y. Yu, S. Tian, I. Petrik, et al., Metalloproteins containing cytochrome, iron–sulfur, or copper redox centers, Chem. Rev. 114 (2014) 4366–4469.
[2] M. Breuer, K.M. Rosso, J. Blumberger, J.N. Butt, Multi-haem cytochromes in *Shewanella oneidensis* MR-1 : structures, functions and opportunities, J. R. Soc. Interface 12 (2015) 1–27.
[3] T.C. Santos, M.A. Silva, L. Morgado, J.M. Dantas, C.A. Salgueiro, Diving into the redox properties of *Geobacter sulfurreducens* cytochromes: a model for extracellular electron transfer, Dalton Trans. 44 (2015) 9335–9344.
[4] B. Kim, C. Leang, Y.R. Ding, H. Glaven, M.V. Coppi, D.R. Lovley, et al., OmcF, a putative *c*-type monoheme outer membrane cytochrome required for the expression of other outer membrane cytochromes in *Geobacter sulfurreducens*, J. Bacteriol. 187 (13) (2005) 4505–4513.
[5] A. Esteve-Núñez, J. Sosnik, P. Visconti, D.R. Lovley, Fluorescent properties of *c*-type cytochromes reveal their potential role as an extracytoplasmic electron sink in *Geobacter sulfurreducens*, Environ. Microbiol. 10 (2008) 497–505.
[6] B. Schuetz, M. Schicklberger, J. Kuermann, A.M. Spormann, J. Gescher, Periplasmic electron transfer via the *c*-type cytochromes MtrA and FccA of *Shewanella oneidensis* MR-1, Appl. Environ. Microbiol. 75 (2009) 7789–7796.
[7] B.A. Methé, K.E. Nelson, J.A. Eisen, I.T. Paulsen, W. Nelson, J.F. Heidelberg, et al., Genome of *Geobacter sulfurreducens*: metal reduction in subsurface environments, Science 302 (2003) 1967–1969.
[8] P.R. Pokkuluri, Y.Y. Londer, N.E.C. Duke, J. Erickson, M. Pessanha, C.A. Salgueiro, et al., Structure of a novel c_7-type three-heme cytochrome domain from a multidomain cytochrome *c* polymer, Protein Sci. 13 (2004) 1684–1692.
[9] P.R. Pokkuluri, Y.Y. Londer, N.E.C. Duke, M. Pessanha, X. Yang, V. Orshonsky, et al., Structure of a novel dodecaheme cytochrome *c* from *Geobacter sulfurreducens* reveals an extended 12 nm protein with interacting hemes, J. Struct. Biol. 174 (2011) 223–233.
[10] M. Assfalg, L. Banci, I. Bertini, M. Bruschi, P. Turano, 800 MHz 1H NMR solution structure refinement of oxidized cytochrome c_7 from *Desulfuromonas acetoxidans*, Eur. J. Biochem. 256 (1998) 261–270.
[11] C.M. Paquete, R.O. Louro, Unveiling the details of electron transfer in multicenter redox proteins, Acc. Chem. Res. 47 (2014) 56–65.
[12] Y.Y. Londer, P.R. Pokkuluri, J. Erickson, V. Orshonsky, M. Schiffer, Heterologous expression of hexaheme fragments of a multidomain cytochrome from *Geobacter sulfurreducens* representing a novel class of cytochromes *c*, Protein Expr. Purif. 39 (2005) 254–260.
[13] E.H. Gordon, E. Steensma, S.J. Ferguson, The cytochrome *c* domain of dimeric cytochrome cd_1 of *Paracoccus pantotrophus* can be produced at high levels as a monomeric holoprotein using an improved *c*-type cytochrome expression system in *Escherichia coli*, Biochem. Biophys. Res. Commun. 281 (2001) 788–794.
[14] E. Arslan, H. Schulz, R. Zufferey, P. Künzler, L. Thöny-Meyer, Overproduction of the *Bradyrhizobium japonicum c*-type cytochrome subunits of the cbb_3 oxidase in *Escherichia coli*, Biochem. Biophys. Res. Commun. 251 (1998) 744–747.
[15] R.T. Francis, R.R. Becker, Specific indication of hemoproteins in polyacrylamide using a double-staining process, Anal. Biochem. 14 (1984) 509–514.
[16] L. Morgado, A.P. Fernandes, Y.Y. Londer, P.R. Pokkuluri, M. Schiffer, C.A. Salgueiro, Thermodynamic characterization of the redox centres in a representative domain of a novel *c*-type multihaem cytochrome, Biochem. J. 420 (2009) 485–492.
[17] C.M. Paquete, D.L. Turner, R.O. Louro, A.V. Xavier, T. Catarino, Thermodynamic and kinetic characterisation of individual haems in multicentre cytochromes c_3, Biochim. Biophys. Acta 1767 (2007) 1169–1179.
[18] M. Dixon, The acceptor specificity of flavins and flavoproteins. I. Techniques for anaerobic spectrophotometry, Biochim. Biophys. Acta 226 (1971) 241–258.
[19] D.O. Lambeth, G. Palmer, The kinetics and mechanism of reduction of electron transfer proteins and other compounds of biological interest by dithionite, J. Biol. Chem. 248 (1973) 6095–6103.
[20] D.L. Turner, C.A. Salgueiro, T. Catarino, J. Legall, A.V. Xavier, NMR studies of cooperativity in the tetrahaem cytochrome c_3 from *Desulfovibrio vulgaris*, Eur. J. Biochem. 241 (1996) 723–731.
[21] R.O. Louro, T. Catarino, C.M. Paquete, D.L. Turner, Distance dependence of interactions between charged centres in proteins with common structural features, FEBS Lett. 576 (2004) 77–80.
[22] B.M. Fonseca, C.M. Paquete, C.A. Salgueiro, R.O. Louro, The role of intramolecular interactions in the functional control of multiheme cytochromes *c*, FEBS Lett. 586 (2012) 504–509.
[23] T. Catarino, D.L. Turner, Thermodynamic control of electron transfer rates in multicentre redox proteins, Chembiochem 2 (2001) 416–424.
[24] R.A. Marcus, N. Sutin, Electron transfers in chemistry and biology, Biochim. Biophys. Acta 811 (1985) 265–322.
[25] C.M. Paquete, I.H. Saraiva, E. Calçada, R.O. Louro, Molecular basis for directional electron transfer, J. Biol. Chem. 285 (2010) 10370–10375.
[26] J.C. Lagarias, J.A. Reeds, M.H. Wright, P.E. Wright, Convergence properties of the Nelder–Mead simplex method in low dimensions, SIAM J. Optim. 9 (1998) 112–147.
[27] C.M. Paquete, R.O. Louro, Molecular details of multielectron transfer: the case of multiheme cytochromes from metal respiring organisms, Dalton Trans. 39 (2010) 4259–4266.
[28] H. Santos, J.J. Moura, I. Moura, J. Legall, A.V. Xavier, NMR studies of electron transfer mechanisms in a protein with interacting redox centres: *Desulfovibrio gigas* cytochrome c_3, Eur. J. Biochem. 141 (1984) 283–296.
[29] C.A. Salgueiro, D.L. Turner, H. Santos, J. LeGall, A.V. Xavier, Assignment of the redox potentials to the four haems in *Desulfovibrio vulgaris* cytochrome c_3 by 2D-NMR, FEBS Lett. 314 (1992) 155–158.
[30] D.L. Turner, C.A. Salgueiro, P. Schenkels, J. LeGall, A.V. Xavier, Carbon-13 NMR studies of the influence of axial ligand orientation on haem electronic structure, Biochim. Biophys. Acta 1246 (1995) 24–28.